MPI-PhT/95-83

Leptoquark Production in $e^-\gamma$ Scattering

Frank Cuypers [1]

cuypers@pss058.psi.de

Max-Planck-Institut für Physik, Werner-Heisenberg-Institut, Föhringer Ring 6, D–80805 München, Germany

Abstract

We perform a model independent analysis of the production of scalar and vector leptoquarks in the $e^-\gamma$ mode of a linear collider of the next generation. Since these leptoquarks are produced singly, higher masses can be probed than in other collider modes, like e^+e^- scattering. We discuss the discovery potential and show how polarization and angular distributions can be used to distinguish between the different types of leptoquarks.

[1] New address as of 1 November 1995: Paul Scherrer Institute, CH-5232 Villigen PSI, Switzerland

1 Introduction

The standard model of strong and electroweak interactions, though extremely successful in describing present day data, is known to be plagued by a number of shortcomings. There is no doubt that it is merely the low energy limit of a more profound underlying theory. In particular, the peculiar similarities between the quark and lepton sectors and their miraculous anomaly cancellations are indicative of a deeper interconnection between these two types of particles.

Many models have been proposed which establish a closer link between quark and lepton degrees of freedom. They generally involve a new class of fields which carry both lepton and baryon number and mediate lepton-quark transitions. Such bosons can come in many combinations of the different quantum numbers and are generically called leptoquarks. They can, for example, emerge as composite scalar or vector states of techni-fermions [1] or preons [2]. Leptoquarks also arize naturally as gauge vectors or Higgs scalars in many grand unified models [3] or superstring-derived models [4].

In principle, e^-p scattering provides the privileged reaction for discovering leptoquarks. Direct searches at HERA [5,6] should be able to exclude leptoquarks below *ca* 300 GeV and a coupling to leptons and quarks above $0.03e$. The LEP-LHC combination could of course extend these limits much further and would also provide a powerful tool for discriminating different leptoquark types [7]. However, today the most stringent limits still originate from low-energy experiments [8]. These bounds could be greatly improved at linear colliders of the next generation, though. In particular, the e^+e^- mode is very promising because it can abundantly pair-produce leptoquarks even if their couplings to leptons and quarks are tiny [9].

In this paper we consider the production of single leptoquarks in $e^-\gamma$ collisions, with laser backscattered photons. This reaction proceeds inevitably via the leptoquark-lepton-quark coupling, and may thus be suppressed if the latter is small. However, it may probe much higher leptoquark masses than the electron-positron annihilation [9] or photon-gluon fusion [6] processes, which necessarily need to produce two leptoquarks. Moreover, since the standard model backgrounds can easily be rendered harmless the data analysis should be exceedingly simple, in contrast to the electron-quark fusion reaction [5]. The angular distributions of the emerging leptoquarks have complicated patterns, which can be used advantageously to tell apart different types of leptoquarks.

The study of scalar leptoquark production in $e^-\gamma$ collisions was first discussed in Ref. [10]. Similarly, vector leptoquarks were considered in Ref. [11]. It was also shown [12] that even kinematically inaccessible scalar leptoquarks can also

be probed this way if their couplings to fermions are large. For lighter scalar leptoquarks, it was pointed out [13] that substantial rates can be obtained even with Weizsäcker-Williams photons in e^+e^- scattering. Because of the hadronic content of the photon, leptoquarks can also be probed via electron-quark fusion in $e^-\gamma$ scattering [14]. It was also shown that this resolved photon contribution may help determining leptoquark properties [15].

In the next section we introduce a model-independent framework for describing a large class of leptoquarks [5] and provide the analytical expressions of the integrated cross sections for producing the various types of leptoquarks. We then shortly review the generation and properties of the photon beam [16]. After this, we discuss the leptoquark discovery potential of $e^-\gamma$ scattering, which is conveniently summarized by Eq. (21). Finally, in the last section we discuss the possibility of determining the nature of the discovered leptoquarks with the help of polarized beams and at hand of their angular distributions.

2 Cross sections

Because of the large number of possible leptoquark types, it is important to perform an analysis which is as model-independent as possible. Therefore, to describe the leptoquark-lepton-quark interactions we use the most general $SU(3)_c \otimes SU(2)_L \otimes U(1)_Y$ invariant effective lagrangian of lowest dimension which conserves lepton (L) and baryon (B) number. It can be separated into two parts, each involving either leptoquarks which carry no fermion number $F = 3B + L = 0$, or leptoquarks with fermion number $F = 2$ [5]:

$$\begin{aligned}\mathcal{L}_{F=0} \;=\;& (h_{2L}\bar{u}_R\ell_L + h_{2R}\bar{q}_L i\sigma_2 e_R)R_2 + \tilde{h}_{2L}\bar{d}_R\ell_L\tilde{R}_2 \\ &+ (h_{1L}\bar{q}_L\gamma^\mu\ell_L + h_{1R}\bar{d}_R\gamma^\mu e_R)U_{1\mu} + \tilde{h}_{1R}\bar{u}_R\gamma^\mu e_R\tilde{U}_{1\mu} \\ &+ h_{3L}\bar{q}_L\boldsymbol{\sigma}\gamma^\mu\ell_L\boldsymbol{U}_{3\mu} \\ &+ \text{ h.c.}\end{aligned} \tag{1}$$

$$\begin{aligned}\mathcal{L}_{F=2} \;=\;& (g_{1L}\bar{q}^c_L i\sigma_2\ell_L + g_{1R}\bar{u}^c_R e_R)S_1 + \tilde{g}_{1R}\bar{d}^c_R e_R\tilde{S}_1 \\ &+ g_{3L}\bar{q}^c_L i\sigma_2\boldsymbol{\sigma}\ell_L\boldsymbol{S}_3 \\ &+ (g_{2L}\bar{d}^c_R\gamma^\mu\ell_L + g_{2R}\bar{q}^c_L\gamma^\mu e_R)V_{2\mu} + \tilde{g}_{2L}\bar{u}^c_R\gamma^\mu\ell_L\tilde{V}_{2\mu} \\ &+ \text{ h.c.}\end{aligned} \tag{2}$$

where the $\boldsymbol{\sigma}$'s are Pauli matrices, while q_L and ℓ_L are the $SU(2)_L$ quark and lepton doublets and u_R, d_R, ℓ_R are the corresponding singlets. The subscripts of the leptoquarks indicates the size of the $SU(2)_L$ representation they belong to. The R- and S-type leptoquarks are spacetime scalars, whereas the U and V are vectors. Family and colour indices are implicit.

Since all these leptoquarks carry an electric charge, they must also couple to the photon. These interactions are described by the kinetic lagrangians for scalar and and vector bosons [6]

$$\mathcal{L}_{J=0} = \sum_{\text{scalars}} \quad (D_\mu \Phi)^\dagger \, (D^\mu \Phi) - m^2 \Phi^\dagger \Phi \tag{3}$$

$$\mathcal{L}_{J=1} = \sum_{\text{vectors}} \quad -\frac{1}{2} \, (D_\mu \Phi^\nu - D_\nu \Phi^\mu)^\dagger \, (D^\mu \Phi_\nu - D^\nu \Phi_\mu) + m^2 \Phi_\mu^\dagger \Phi^\nu \tag{4}$$

with the covariant derivative

$$D_\mu = \partial_\mu - ieQA_\mu \ , \tag{5}$$

where Φ and A are the leptoquark and photon fields, m and Q are the leptoquark mass and electromagnetic charge and e is the electromagnetic coupling constant. This lagrangian describes the minimal vector boson coupling, typical of a composite leptoquark. If, however, the vector leptoquarks are gauge bosons, an extra Yang-Mills piece has to be added in order to maintain gauge invariance [6]:

$$\mathcal{L}_G = \sum_{\text{vectors}} \quad -ie \ \Phi_\mu^\dagger \Phi_\nu \, (\partial^\mu A^\nu - \partial^\nu A^\mu) \ . \tag{6}$$

Ignoring the resolved photon contributions, the following leptoquark reactions are possible to lowest order in $e^-\gamma$ collisions:

$$F = 0 : \begin{cases} J = 0 : & \begin{cases} e_R^- \, \gamma \to u_L \ R_2^{-5/3} & e_L^- \, \gamma \to u_R \ R_2^{-5/3} \\ \qquad\quad d_L \ R_2^{-2/3} & \qquad\quad d_R \ \tilde{R}_2^{-2/3} \end{cases} \\ J = 1 : & \begin{cases} e_R^- \, \gamma \to u_R \ \tilde{U}_1^{-5/3} & e_L^- \, \gamma \to u_L \ U_3^{-5/3} \\ \qquad\quad d_R \ U_1^{-2/3} & \qquad\quad d_L \ U_1^{-2/3} \\ & \qquad\quad d_L \ U_3^{-2/3} \end{cases} \end{cases}$$

$$
F=2:\;\begin{cases} J=0:\; \begin{cases} e^-_R\,\gamma \to \bar{u}_R\; S_1^{-1/3} & e^-_L\,\gamma \to \bar{u}_L\; S_1^{-1/3} \\ \qquad\qquad \bar{d}_R\; \tilde{S}_1^{-4/3} & \qquad\qquad \bar{u}_L\; S_3^{-1/3} \\ & \qquad\qquad \bar{d}_L\; S_3^{-4/3} \end{cases} \\ J=1:\; \begin{cases} e^-_R\,\gamma \to \bar{u}_L\; V_2^{-1/3} & e^-_L\,\gamma \to \bar{u}_R\; \tilde{V}_2^{-1/3} \\ \qquad\qquad \bar{d}_L\; V_2^{-4/3} & \qquad\qquad \bar{d}_R\; V_2^{-4/3} \end{cases} \end{cases}
$$

The superscripts of the leptoquarks indicate their electromagnetic charge. The typical s-, t- and u-channel Feynman diagrams for the $F = 0$ and $F = 2$ leptoquark production are shown in Fig. 1. The cross sections, though, do not depend explicitly on this quantum number.

There are 24 different types of processes, depending on whether the produced leptoquark is a scalar, vector or gauge boson, whether it couples to right- or left-handed leptons and what is its electromagnetic charge ($Q = -1/3, -2/3, -4/3, -5/3$). The differential cross sections are lengthy and we do not report them here. We agree with the unpolarized expressions reported in Refs [10,11,12] [2], though.

Let us define

$$
x = \frac{m^2}{s}\;, \tag{7}
$$

where m is the leptoquark mass and s is the centre of mass energy squared. We also use the generic leptoquark coupling λ to the electrons and quarks, and denote the electron and photon polarizations P_e and P_γ. We find for the integrated scalar cross sections

$$
\begin{aligned}
\sigma(J=0) \quad = \quad & \frac{3\pi\alpha^2}{2s} \quad \left(\frac{\lambda}{e}\right)^2 \quad \frac{1 \pm P_e}{2} \quad \times \\
& \Big\{ \quad \Big(-(3+4Q) + \left(7+8Q+8Q^2\right) x\Big) \quad (1-x) \\
& \quad +4Q\,(Q-(2+Q)\,x) \quad x\ln x \\
& \quad -2\,(1+Q)^2\left(1-2x+2x^2\right) \quad \ln\frac{m_q^2/s}{(1-x)^2} \\
& \pm P_\gamma \Big[\Big(-\left(7+12Q+4Q^2\right)+3x\Big) \quad (1-x) \\
& \quad +4Q^2 \quad x\ln x
\end{aligned} \tag{8}
$$

[2] The colour factor is not explicitly stated in Refs [10,12].

$$-2\left(1+Q\right)^2\left(1-2x\right) \quad \ln\frac{m_q^2/s}{\left(1-x\right)^2} \quad \Big] \quad \Big\} \, .$$

The unpolarized part ($P_e = P_\gamma$=0) of this expression agrees with the result reported in Ref. [13], up to the colour factor, which we include explicitly here. The vector cross sections are

$$\begin{aligned}
\sigma(J=1) \quad &= \quad \frac{3\pi\alpha^2}{8m^2} \quad \left(\frac{\lambda}{e}\right)^2 \quad \frac{1\pm P_e}{2} \quad \times \qquad (9)\\
&\Big\{ \quad \left(Q^2+\left(8-16Q-Q^2\right)x+8\left(7+8Q+8Q^2\right)x^2\right) \quad (1-x)\\
&\quad -4Q\left(Q+\left(8+3Q\right)x-8Qx^2+8\left(2+Q\right)x^3\right) \quad \ln x\\
&\quad -16\left(1+Q\right)^2\left(1-2x+2x^2\right) \quad x\ln\frac{m_q^2/s}{\left(1-x\right)^2}\\
&\pm P_\gamma \Big[\ \left(-3Q^2+\left(40+48Q+63Q^2\right)x+24x^2\right) \quad (1-x)\\
&\quad -4Q\left(-3Q+8\left(3+Q\right)x\right) \quad x\ln x\\
&\quad +16\left(1+Q\right)^2\left(1-2x\right) \quad x\ln\frac{m_q^2/s}{\left(1-x\right)^2} \quad \Big] \quad \Big\} \, .
\end{aligned}$$

Finally, if the vector is a gauge field, we have

$$\begin{aligned}
\sigma^{\rm YM}(J=1) \quad &= \quad \frac{3\pi\alpha^2}{m^2} \quad \left(\frac{\lambda}{e}\right)^2 \quad \frac{1\pm P_e}{2} \quad \times \qquad (10)\\
&\Big\{ \quad \left(4Q^2+\left(1-4Q\right)x+\left(7+8Q+8Q^2\right)x^2\right) \quad (1-x)\\
&\quad -4Q\left(2-Qx+\left(2+Q\right)x^2\right) \quad x\ln x\\
&\quad -2\left(1+Q\right)^2\left(1-2x+2x^2\right) \quad x\ln\frac{m_q^2/s}{\left(1-x\right)^2}\\
&\pm P_\gamma \Big[\ \left(\left(5+4Q+12Q^2\right)+3x\right)x \quad (1-x)\\
&\quad +4Q\left(Q-\left(4+Q\right)x\right) \quad x\ln x\\
&\quad +2\left(1+Q\right)^2\left(1-2x\right) \quad x\ln\frac{m_q^2/s}{\left(1-x\right)^2} \quad \Big] \quad \Big\} \, .
\end{aligned}$$

The electron and quark masses have been set equal to zero everywhere to derive Eqs (8-10), except in the squared u-channel matrix elements. It is essential to perform the calculation of these terms with a finite quark mass, because it regulates the singularity which occurs when a leptoquark is emitted in the direction of the incoming electron. The approximation $\ln m_q^2/s/(1-x)^2$ we have written for this u-channel logarithm stays more than accurate up to within a few quark masses from the threshold. It is straightforward to compute

the full expression [13]. Moreover, the integration in the backward direction introduces non-vanishing contributions of the order $\mathcal{O}(m_q^2/m_q^2)$ to the non-logarithmic parts of the cross sections (8-10) [3].

The threshold behaviour of the cross sections, around $x = 1$, mainly depends on the u-channel singularity and on the electron and photon relative polarizations:

$$x = 1 : \begin{cases} \sigma(J=0) & \propto & (1+Q)^2 & (1 \mp P_\gamma)(1 \pm P_e) \\ \\ \sigma(J=1) & \propto & 2(1+Q)^2 & (1 \pm P_\gamma)(1 \pm P_e) \end{cases} \tag{11}$$

The scalar cross section quickly drops to zero for like-sign initial state electrons and photons polarizations, whereas the vector cross section is suppressed when these polarizations have opposite signs. For equal couplings, the vector threshold cross sections are twice as intense as the scalar ones.

In the asymptotic region, for $x = 0$, the $J = 0$ and $J = 1$ leptoquarks also display very different behaviours. Whereas the scalar cross sections decrease like $1/s$, the vector cross sections eventually increase like $\ln s$. If the vectors are gauge fields, though, their cross sections saturate for large values of s.

3 Photon Beams

The cross sections (8-10) still have to be folded with a realistic Compton backscattered photon spectrum [16]:

$$\sigma(s) = \int_{x_{\min}}^{x_{\max}} \mathrm{d}x \frac{\mathrm{d}n(x)}{\mathrm{d}x} \sigma(xs) \ , \tag{12}$$

where the probability density of a photon to have the energy fraction $x = E_\gamma / E_{\mathrm{beam}}$ is given by

$$\begin{aligned} \frac{\mathrm{d}n(x)}{\mathrm{d}x} = \frac{1}{\mathcal{N}} \Bigg\{ & 1 - x + \frac{1}{1-x} - \frac{4x}{z(1-x)} + \frac{4x^2}{z^2(1-x)^2} \\ & + P_{\mathrm{beam}} P_{\mathrm{laser}} \frac{x(2-x)}{1-x} \left[\frac{2x}{z(1-x)} - 1 \right] \Bigg\} \ , \end{aligned} \tag{13}$$

[3] I am very much indebted to David London and Hélène Nadeau for pointing this out to me.

where

$$\mathcal{N} = \frac{z^3 + 18z^2 + 24z + 8}{2z(z+1)^2} + \left(1 - \frac{4}{z} - \frac{8}{z^2}\right)\ln(1+z) \qquad (14)$$
$$+ P_{\rm beam}P_{\rm laser}\left[2 - \frac{z^2}{(z+1)^2} - \left(1 + \frac{2}{z}\right)\ln(1+z)\right] \ ,$$

$$z = \frac{4E_{\rm beam}E_{\rm laser}}{m_e^2} \ , \qquad (15)$$

m_e being the mass of the electron,

By design, the energy fraction x of the photons is limited from above to

$$x_{\rm max} = \frac{2+2\sqrt{2}}{3+2\sqrt{2}} \approx 0.8284 \qquad (16)$$

in order to prevent electron-positron pair-production from photon rescattering. In practice, it is also limited from below, because only the harder photons are produced at a small angle with respect to the beam-pipe according to

$$\theta_\gamma(x) \simeq \frac{m_e}{E_{\rm beam}}\sqrt{\frac{z}{x} - z - 1} \ . \qquad (17)$$

The softer photons are emitted at such large angles that they are bound to miss the opposite highly collimated electron beam. Assuming a conversion distance of *ca* 5 cm and a beam size of 500 nm diameter, the lower bound we adopt for the photon energy fraction is

$$x_{\rm min} = .5 \ . \qquad (18)$$

Of course, if the beams are very flat, this cut-off will be somewhat softened out. However, in the threshold region is has no effect. When it sets in, at $s = m^2/x_{\rm min} = 2m^2$, it is visible on the plots of Fig. 3 as a slight kink in the slopes.

The polarization of the backscattered photons is given by

$$P_\gamma(x) = \frac{P_{\rm laser}\zeta(2 - 2x + x^2) + P_{\rm beam}x(1+\zeta^2)}{(1-x)(2-2x+x^2) - 4x(z - zx - x)/z^2 - P_{\rm beam}P_{\rm laser}\zeta x(2-x)} \ , \qquad (19)$$

with

$$\zeta = 1 - x(1 + 1/z) \ . \qquad (20)$$

All these features of the Compton backscattered photon beams are displayed in Fig. 2. In particular, it appears that if the signs of the polarizations of the laser and the Compton scattered electron beams are chosen to be opposite, we obtain the most intense, hard and highly polarized photon beam. We adopt this choice throughout the rest of this paper.

4 Leptoquark Discovery Limits

To present our results, we have chosen to work with a quark mass in the u-channel propagator $m_q = 10$ MeV. Since the dependence of the cross sections on this mass is only logarithmic, the error does not exceed a few % and is mainly confined to the immediate threshold region. We also assumed both the unaltered and the Compton scattered electron beams to be 90% polarized. This should be fairly easy to realize at a linear collider of the next generation.

In Fig. 3 we have displayed the behaviours of the cross sections (8-10) as functions of the collider centre of mass energy. For the purpose of these plots, we have set the leptoquark-electron-quark coupling equal to the electromagnetic coupling constant $\lambda = e$.

In general, leptoquarks which are produced in the reactions (8-10), will decay into a charged lepton and a jet with a substantial branching ratio. If the leptoquarks are bound to a single generation, the decay lepton is an electron. Around threshold, the u-channel pole is dominant, so the quarks and leptoquarks are mostly produced at very small angles from the beampipe. Since the leptoquarks are almost at rest, most of the electron and quark into which they decay are emitted at large angles. The leptoquark signature is thus a low transverse momentum (or even invisible) jet, and a high transverse momentum electron and jet pair whose invariant mass is closely centered around the leptoquark mass. Away from threshold, the u-channel is no longer dominant, and the leptoquark signature becomes a high transverse momentum electron and pair of jets, where the electron and one of the jets have a combined invariant mass close to the leptoquark mass.

If all jet pairs with an invariant mass around the Z^0 mass are cut out, there is no Z^0 Compton scattering background. The next order background which then subsists is the quark photoproduction process $e^-\gamma \to e^- q\bar{q}$. This background, though, will not show any peak in the electron-jet invariant mass distribution at the leptoquark mass, and can moreover be drastically reduced by requiring a minimum transverse momentum for the electron. If one allows for leptoquarks which couple equally well to different generations, the final state can contain a muon instead of an electron. In this case, of course, there is no standard model background at all.

To estimate the leptoquark discovery potential of $e^-\gamma$ collisions, we have plotted in Fig. 4 the boundary in the $(m_{LQ}, \lambda/e)$ plane, below which the cross section $\sigma(J=1, Q=-5/3)$ in Eq. (10) yields less than 10 events. For this we consider four different collider energies and assume 10 fb^{-1} of accumulated luminosity. In general, as can be inferred from Eq. (11), these curves are closely osculated by the relation

$$\frac{\lambda}{e} \quad = \quad 0.03 \quad \frac{m/\mathrm{TeV}}{\sqrt{\mathcal{L}/\mathrm{fb}^{-1}}} \quad \sqrt{\frac{n}{(J+1)(1+Q)^2}} \qquad (m \leq .8\sqrt{s_{ee}}) \ , \quad (21)$$

where λ is the leptoquark's coupling to leptons and quarks, m its mass, Q its charge, J its spin, n is the required number of events and $\mathcal{L}$ is the available luminosity. This scaling relation provides a convenient means to gauge the leptoquark discovery potential of $e^-\gamma$ scattering. It is valid for leptoquark masses short off 80% of the collider energy and assumes the electron beams to be 90% polarized ($|P_e| = .9$) while the chirality of the fully polarized photon beam is chosen such as to enhance the threshold cross section (*cf.* Eq. (11)).

In comparison, the best bounds on the leptoquark couplings which have been derived indirectly from low energy data [8] are no better than

$$\frac{\lambda}{e} \quad \geq \quad m/\mathrm{TeV} \ , \qquad (22)$$

for leptoquark interactions involving only the first generation. Similar bounds on couplings involving higher generations are even poorer.

5 Leptoquark-Type Discrimination

If a leptoquark is discovered someday, it is interesting to determine its nature. In principle, $e^-\gamma$ scattering may discriminate between the 24 combinations of the quantum numbers J, Q and P, where the latter is the chirality of the electron to which the leptoquark couples. For the case $J = 1$ we make the distinction between gauge and non-gauge leptoquarks.

It is of course trivial to determine P by switching the polarization of the electron beam. Similarly, it is almost as easy to distinguish scalars from vectors. Indeed, as can be inferred from Eqs (11) and from Fig. 3, all threshold cross sections are very sensitive to the relative electron and photon polarizations. Since this effect works in opposite directions for $J = 0$ and $J = 1$, a simple photon polarization flip upon discovery should suffice to determine the spin of the discovered leptoquarks.

Determining the other quantum numbers, unfortunately, is not as easy. In practice this task is not facilitated by the fact all the different models involving leptoquarks predict very different values for their couplings to leptons and quarks, if at all. Basically, we have no idea what to expect. Fig. 3 indicates that it may be possible to discriminate some of the different vector leptoquarks, by combining the information gathered from polarization flips and an energy scan. It will, however, be exceedingly difficult to differentiate for instance the different scalar leptoquarks from eachother using the information from total cross sections alone.

Much more discriminating power can be obtained from the differential distributions, though. We do not report their long analytical forms here. As it turns out, the interferences between the different channels result into rather complex angular dependences of the cross sections. There are even radiation zeros for the reactions involving scalar and Yang-Mills leptoquarks of charges -1/3 and -2/3. Note that in the cross-channel reaction $e^- q \to LQ\gamma$ these radiation zeros occur for the scalar and Yang-Mills leptoquarks of charges -4/3 and -5/3 [7].

These very salient features could well be observed away from threshold, where the u-channel pole is no longer so dominant. Of course, the convolution with the photon energy and polarization spectra washes out to some extent these prominent features. But, as can be gathered from Fig. 5, even so the angular distributions of the different leptoquarks retain their distinctive characteristics. In this figure, we have considered 400 GeV leptoquarks produced at a 1 TeV collider.

To roughly estimate the $e^-\gamma$ potential for discriminating the different types of leptoquarks, we compare these differential distributions with a Kolmogorov-Smirnov test. Say a and b are two different kinds of leptoquarks and a is the one which is observed. The probability that b could be mistaken for a is related to the statistic

$$D \;=\; \sqrt{N_a}\;\sup\left|\frac{1}{\sigma_a}\int^{\theta}\mathrm{d}\theta\frac{\mathrm{d}\sigma_a}{\mathrm{d}\theta}-\frac{1}{\sigma_b}\int^{\theta}\mathrm{d}\theta\frac{\mathrm{d}\sigma_b}{\mathrm{d}\theta}\right|\;, \tag{23}$$

where θ is the polar angle of the leptoquark and $N_a = \mathcal{L}\sigma_a$ is the number of observed events.

Focusing on the case of Fig. 5, where a 400 GeV leptoquark is studied at a 1 TeV collider, Tables 1 and 2 summarize the minimal values of

$$\frac{\lambda}{e}\quad\sqrt{\mathcal{L}/\mathrm{fb}^{-1}}$$

needed to tell apart two different types of leptoquarks with 99.9% confidence,

i.e., setting $D = 1.95$ in Eq. (23). Assuming each combination of electron and photon polarizations has accumulated 50 fb^{-1} of data, some leptoquark types have so different angular distributions that a coupling as small as $\lambda = .0085e$ is quite sufficient to tell them apart. Others need as much as $\lambda = .31e$. Obviously, these numbers are only valid for this particular choice of leptoquark mass and collider energy, and could be improved with a more sophisticated analysis. Nevertheless, they should be indicative of what resolving power an $e^-\gamma$ scattering experiment can achieve.

6 Conclusions

We have studied leptoquark production in the $e^-\gamma$ mode of a linear collider of the next generation. To perform this analysis, we have considered all types of scalar and vector leptoquarks, whose interactions with leptons and quarks conserve lepton and baryon number and are invariant under the standard model $SU(3)_c \otimes SU(2)_L \otimes U(1)_Y$ gauge group. For the vectors we distinguish between leptoquarks which couple minimally to photons and Yang-Mills fields.

The advantage of an $e^-\gamma$ experiment over, *e.g.*, e^+e^- annihilation is that the leptoquarks need not be produced in pairs. Hence higher masses can be explored. The disadvantage is that the $e^-\gamma$ reactions proceed only via the *a priori* unknown leptoquark-lepton-quark couplings.

The standard model backgrounds can be reduced to almost zero by simple kinematical cuts, and the discovery potential is conveniently summarized by the scaling relation Eq. (21). The spin of the leptoquarks can easily be determined at threshold by inverting the polarization of the photon beam. Moreover, each leptoquark type displays very characteristic angular distributions, some of which having even radiation zeros. Therefore, the prospects for discriminating different leptoquarks of the same spin can be greatly enhanced by studying angular correlations.

All our results have been obtained with a realistic electron beam polarization and Compton backscattered photon spectra.

Acknowledgement

It is a pleasure to thank Stan Brodsky and Clem Heusch for their hospitality at SLAC and UCSC, where this project was initiated. Many fruitful discussions with Sacha Davidson, Paul Frampton, Slava Ilyin, David London and Hélène Nadeau are gratefully acknowledged. I am also particularly indebted to David

London for pointing out Refs [10,11,12,13,14,15] to me and to Hélène Nadeau for helping me eliminate an error from my calculations.

References

[1] see, *e.g.*, S. Dimopoulos, J. Ellis, *Nucl. Phys.* **B182** (1981) 505;
O. Shenkar, *Nucl. Phys.* **B206** (1982) 253.

[2] see, *e.g.*, W. Buchmüller, *Phys. Lett.* **B145** (1984) 151;
B. Schrempp, F. Schrempp, *Phys. Lett.* **B153** (1985) 101.

[3] see, *e.g.*, P.H. Frampton, *Mod. Phys. Lett.* **A7** (1992) 559.

[4] see, *e.g.*, J. Hewett, T. Rizzo, *Phys. Rep.* **183** (1989) 193.

[5] W. Buchmüller, R. Rückl, D. Wyler, *Phys. Lett.* **B191** (1987) 442.

[6] J. Blümlein, E. Boos, A. Pukhov, *Mod. Phys. Lett.* **A9** (1994) 3007 [hep-ph/9404321].

[7] V. Ilyin *et al.*, *Phys. Lett.* **B351** (1995) 504 (*err.* **B352** (1995) 500), *ibid.* **B356** (1995) 531.

[8] S. Davidson, D. Bailey, B. Campbell, *Z. Phys.* **C61** (1994) 613 [hep-ph/9309310];
M. Leurer, *Phys. Rev.* **D49** (1994) 333 [hep-ph/9309266], *ibid.* **D50** (1994) 536 [hep-ph/9312341].

[9] J. Blümlein, R. Rückl, *Phys. Lett.* **B304** (1993) 337;
D. Choudhury *Phys. Lett.* **B346** (1995) 291 [hep-ph/9408250].

[10] J.L. Hewett, S. Pakvasa, *Phys. Lett.* **B227** (1989) 178.

[11] J.E. Cieza Montalvo, O.J.P. Éboli, *Phys. Rev.* **D47** (1993) 837 [hep-ph/9208242].

[12] H. Nadeau, D. London, *Phys. Rev.* **D47** (1993) 3742 [hep-ph/9303238].

[13] G. Bélanger, D. London and H. Nadeau, *Phys. Rev.* **D49** (1994) 3140 [hep-ph/9307324].

[14] T.M. Aliev, Kh.A. Mustafaev, *Sov. J. Nucl. Phys.* **53** (1991) 482;
O.J.P. Éboli *et al.*, *Phys. Lett.* **B311** (1993) 147 [hep-ph/9306229];
M.A. Doncheski, S. Godfrey, *Phys. Rev.* **D49** (1994) 6220 [hep-ph/9311288].

[15] M.A. Doncheski, S. Godfrey, *Phys. Rev.* **D51** (1995) 1040 [hep-ph/9407317].

[16] I.F. Ginzburg, G.L. Kotkin, V.G. Serbo, V.I. Telnov, *Nucl. Instr. Meth.* **205** (1983) 47.

$\frac{\lambda}{e}\sqrt{\mathcal{L}/\mathrm{fb}^{-1}}$			$J=0$			
			$F=0$		$F=2$	
			$Q=-\frac{5}{3}$	$Q=-\frac{2}{3}$	$Q=-\frac{4}{3}$	$Q=-\frac{1}{3}$
$J=0$	$F=0$	$Q=-\frac{5}{3}$	$\times$	.2	.7	.2
		$Q=-\frac{2}{3}$	.8	$\times$	.6	2.2
	$F=2$	$Q=-\frac{4}{3}$	1.1	.3	$\times$	.3
		$Q=-\frac{1}{3}$	.4	1.0	.3	$\times$

Table 1
Smallest values of $\lambda/e\sqrt{\mathcal{L}/\mathrm{fb}^{-1}}$ which allow discriminating with 99.9% confidence two different 400 GeV scalar leptoquarks at a 1 TeV collider. The leptoquarks listed in the rows are assumed to produce the data, whereas those listed in the columns are tested against this data.

$\frac{\lambda}{e}\sqrt{\mathcal{L}/\mathrm{fb}^{-1}}$			$J=1$				$J=1$ YM field			
			$F=0$		$F=2$		$F=0$		$F=2$	
			$Q=-\frac{5}{3}$	$Q=-\frac{2}{3}$	$Q=-\frac{4}{3}$	$Q=-\frac{1}{3}$	$Q=-\frac{5}{3}$	$Q=-\frac{2}{3}$	$Q=-\frac{4}{3}$	$Q=-\frac{1}{3}$
$J=1$	$F=0$	$Q=-\frac{5}{3}$	$\times$	.3	.8	.1	.3	.2	.3	.1
		$Q=-\frac{2}{3}$	.9	$\times$	.7	.8	.5	.5	.5	.5
	$F=2$	$Q=-\frac{4}{3}$	1.2	.3	$\times$	.2	.6	.3	.5	.1
		$Q=-\frac{1}{3}$	.3	.5	.2	$\times$	.2	.2	.2	.9
$J=1$ YM field	$F=0$	$Q=-\frac{5}{3}$	.2	.1	.3	.07	$\times$	.2	.8	.06
		$Q=-\frac{2}{3}$	.6	.4	.6	.3	1.0	$\times$	.9	.3
	$F=2$	$Q=-\frac{4}{3}$	.3	.1	.3	.09	1.1	.3	$\times$	.08
		$Q=-\frac{1}{3}$	.2	.4	.2	1.0	.2	.2	.2	$\times$

Table 2
Same as Table 1 for the vector leptoquarks. Scalar and vector leptoquarks can easily be told apart by flipping the laser polarization at threshold.

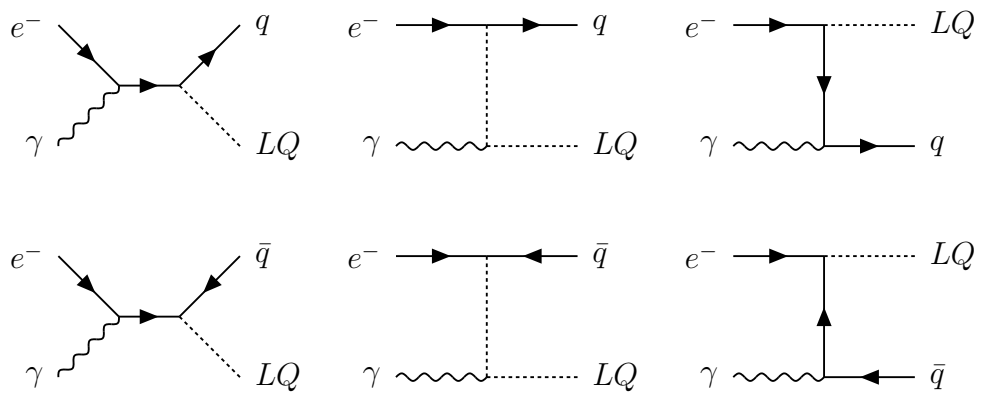

Fig. 1. Lowest order Feynman diagrams for the production of $F = 0$ (upper graphs) and $F = 2$ (lower graphs) leptoquarks.

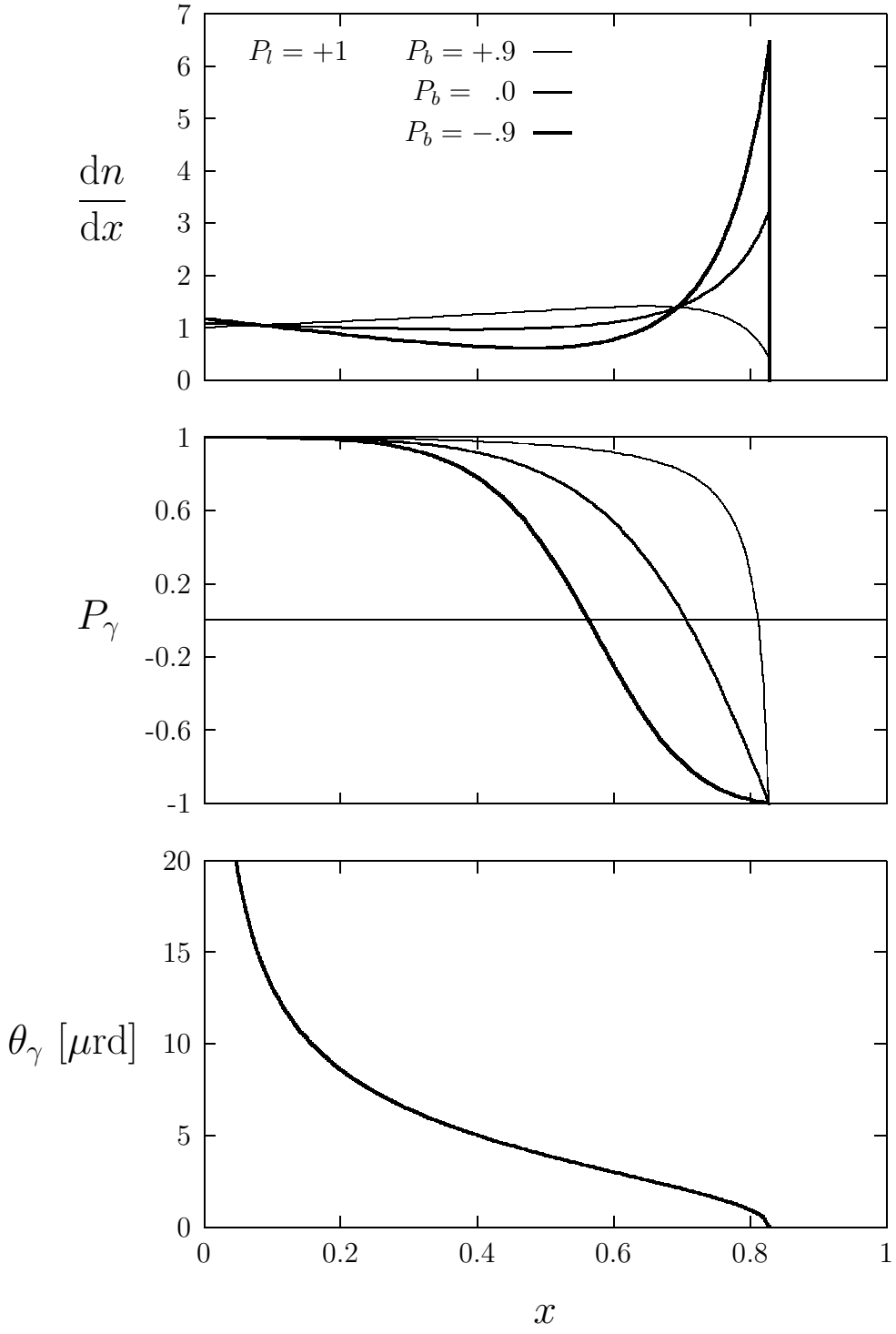

Fig. 2. Back-scattered photon energy spectrum, polarization and polar angle as functions of $x = E_\gamma/E_{\mathrm{beam}}$ for three different combinations of beam polarizations.

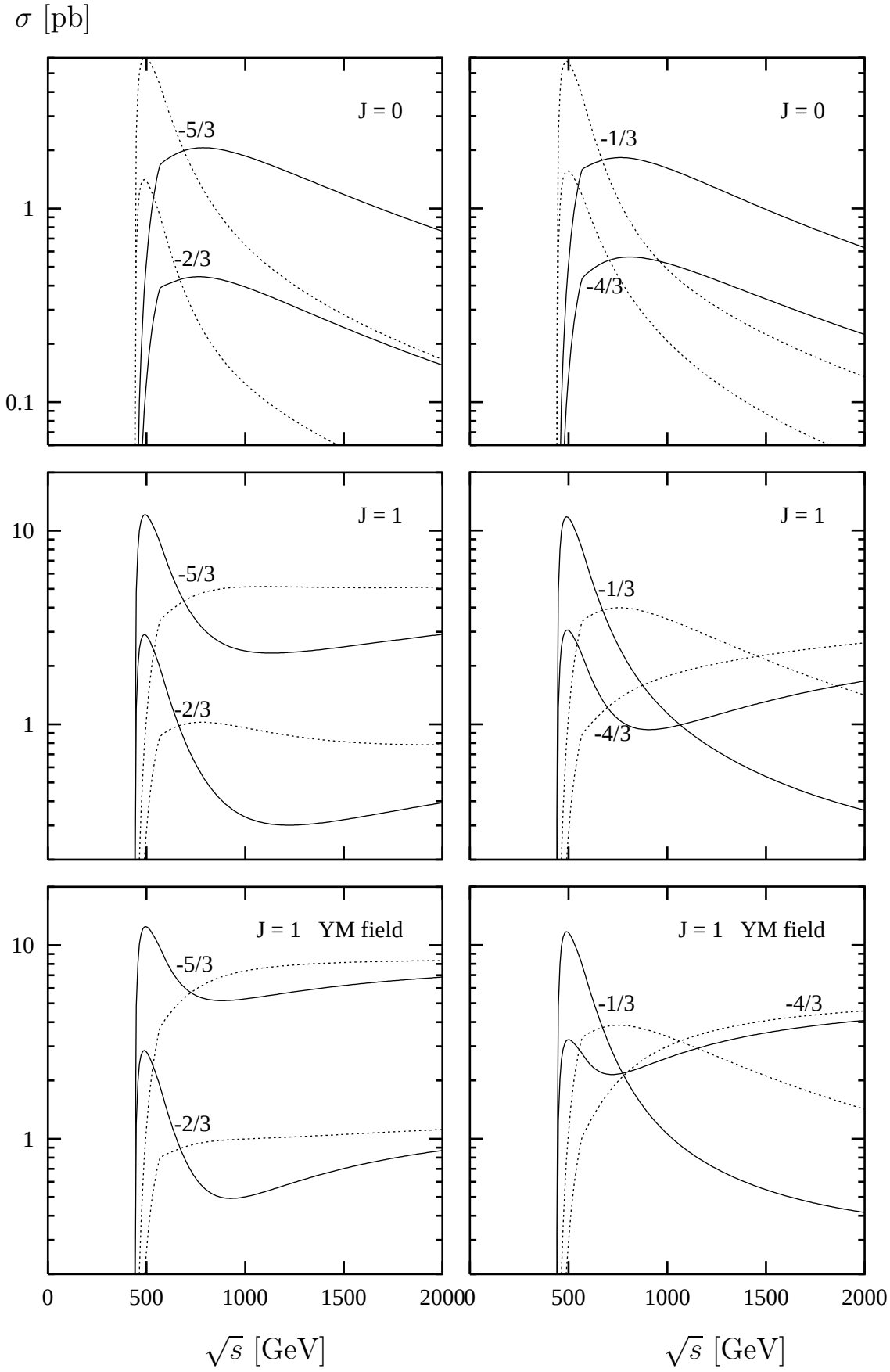

Fig. 3. Dependence of the leptoquark production cross section on the collider energy. The leptoquark mass is 400 GeV. The electron beams are 90% polarized ($|P_e| = .9$). The polarization of the photons depends on their energy fraction and is given by Eq. (19). The solid curves correspond to the choice of photon and electron polariza-

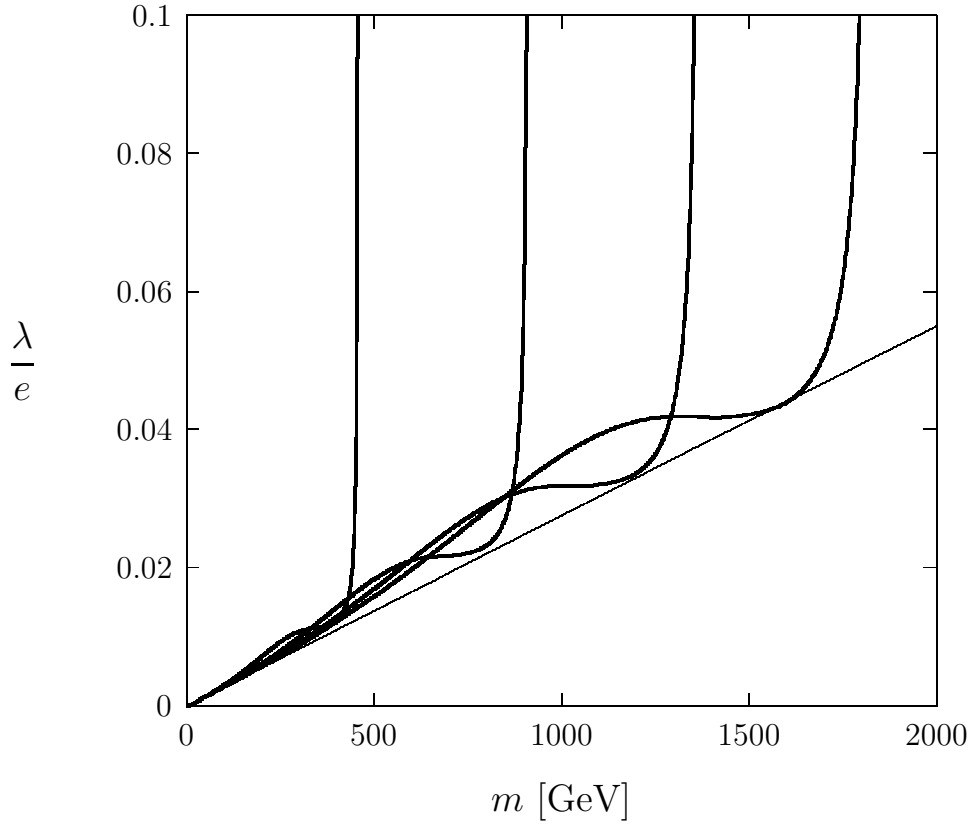

Fig. 4. Loci of $\sigma(J = 1, Q = -5/3) = 1$ fb as a function of the leptoquark mass and coupling to fermions. The polarizations are $|P_e| = .9$ and $\langle P_e P_\gamma \rangle > 0$. The collider energies are from left to right .5, 1, 1.5 and 2 TeV. The thinner osculating line is given by Eq. (21).

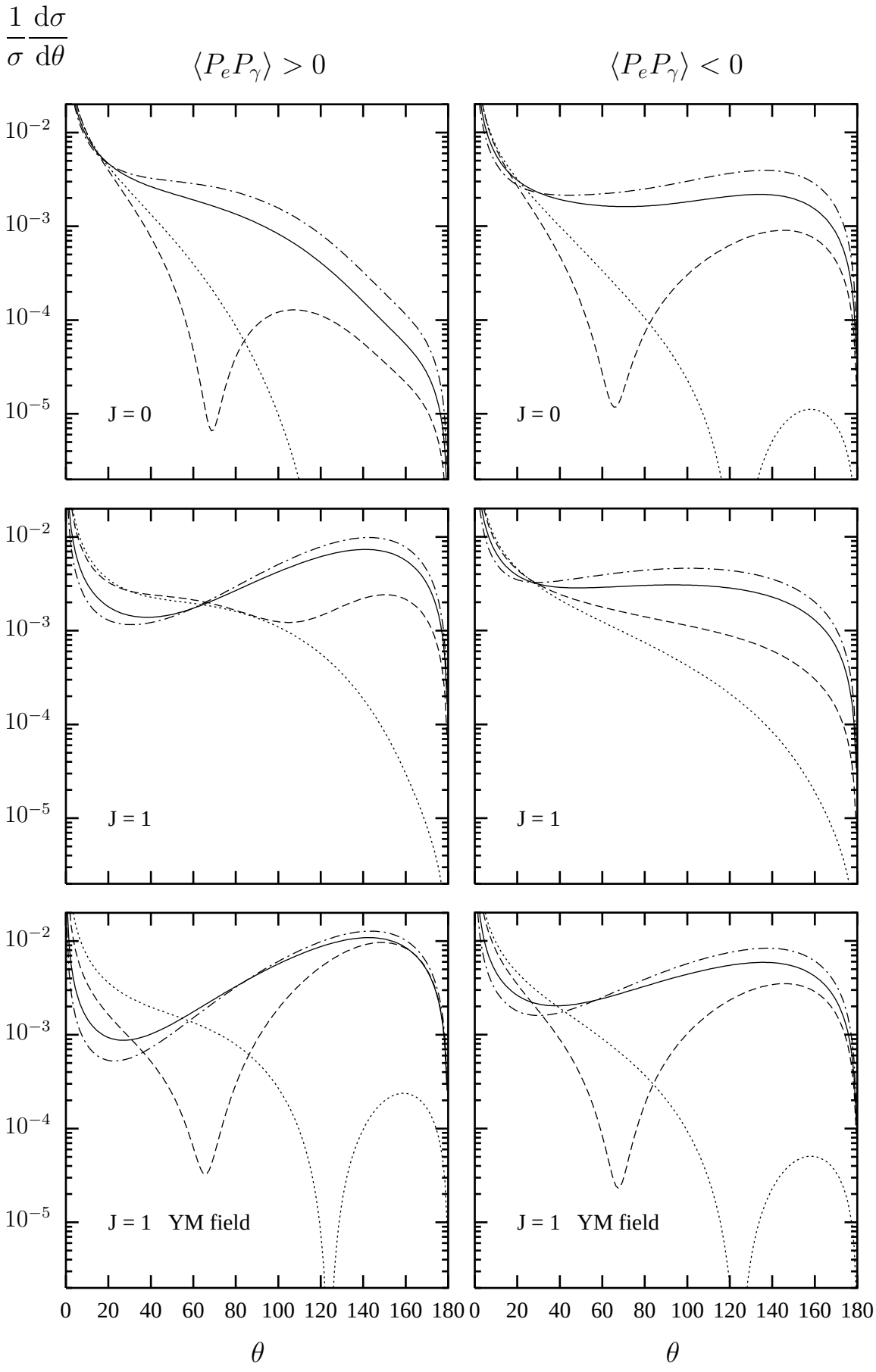

Fig. 5. Angular distribution of the leptoquark production cross section. The plotted angle is spanning the directions of the incoming electron and the outgoing leptoquark. The collider energy is 1 TeV and the leptoquark mass is 400 GeV. The coding